Applied Ocean Research 52 (2015) 212–221

Contents lists available at ScienceDirect

Applied Ocean Research

journal homepage: www.elsevier.com/locate/apor

Parametric estimation of ship maneuvering motion with integral sample structure for identification

Cao Jian [a], Zhuang Jiayuan [a,*], Xu Feng [b], Yin Jianchuan [c], Zou Zaojian [d,e], Yu Hao [f], Xiao Tao [b], Yang Luchun [b]

[a] Science and Technology on Underwater Vehicle Laboratory, Harbin Engineering University, Harbin 150001, Heilongjiang, China
[b] Wuhan Second Ship Design and Research Institute, Wuhan 430064, Hubei, China
[c] Navigation College, Dalian Maritime University, Dalian 116026, Liaoning, China
[d] School of Naval Architecture, Ocean and Civil Engineering, Shanghai Jiao Tong University, Shanghai 200240, China
[e] State Key Laboratory of Ocean Engineering, Shanghai Jiao Tong University, Shanghai 200240, China
[f] China Ship Research and Development Academy, Beijing 100192, China

ARTICLE INFO

Article history:
Received 8 January 2015
Received in revised form 28 April 2015
Accepted 13 June 2015
Available online 10 July 2015

Keywords:
Ship maneuvering motion
Sample structure for identification
Support vector machines
System identification

ABSTRACT

This documentation presents the parametric identification modeling of ship maneuvering motion with integral sample structure for identification (ISSI) and Euler sample structure for identification (ESSI) based on least square support vector machines (LS-SVM), where ISSI is used for the construction of in–out sample pairs. By using *Mariner Class Vessel*, the sample dataset are obtained from 15°/15° zigzag maneuvering simulation based on Abkowitz model. By analyzing the simulation data including rudder angle, surge velocity, sway velocity, yaw rate and so forth, the hydrodynamic derivatives in Abkowitz model are all identified. The validation of the proposed identification algorithm is verified by the high precisions of the identified hydrodynamic derivatives and maneuvering prediction results. The comparison is also conducted between the proposed ISSI and the conventional Euler sample structure for identification (ESSI), and the experimental results shows that ISSI is much more appropriate for parametric identification modeling of ship maneuvering motion.

1. Introduction

System identification (SI) in combination with free-running model tests or full-scale trials is known as an efficient technique for ship maneuvering modeling in recent decades. Consequently, some researchers have devoted themselves to this work, and some identification techniques are developed. Up to date, various identification algorithms have been employed to identify the hydrodynamic derivatives in the mathematical model of ship maneuvering motion. The classical methods include least square method (LS) [1,2], extended Kalman filter (EKF) [3,4], model reference method (MR), recursive prediction error method (RPE) [5,6], maximum likelihood method (ML) [7] etc. as well as their improved ones [8]. To overcome the inherent defects of the classical SI methods, i.e., dependency on initial values, ill-conditioned solutions and simultaneous drift, frequency domain identification method [9–11], neural network (NN) and support vector machines (SVM) are proposed for parametric identification.

NN and SVM are considered as the typical representation of artificial intelligence algorithms and the modern identification techniques. As a matter that NN is accomplished in nonlinear regression, it is commonly adopted for black-box modeling of ship maneuvering motion [12–17], whereas it is rarely taken into consideration for parametric identification. In contrast, SVM not only can be used for black-box modeling [18], but also adept at approximation of the hydrodynamic derivatives in the mathematical model via the switch of kernel function, i.e., commonly linear kernel function for parametric identification while radius basis function kernel function for nonlinear regression.

SVM was proposed by Vapnik in 1990s [19], and afterwards it has been widely developed and improved to solve classification and regression problems for a large number of scientific and engineering areas [20,21]. It was firstly introduced into the area of ship maneuvering modeling by Luo and Zou [22]. In this literature, least square SVM (LS-SVM) is employed to identify the hydrodynamic derivatives in Abokowitz model based on the data simulated with Mariner Class Vessel. Thereafter, Zhang and Zou verified the validation of ε-SVM in completing the similar mission [23]. Zhang and Zou also applied ε-SVM to dealing with the data obtained from captive model tests, and satisfactory results were gained [24]. Xu and

* Corresponding author. Tel.: +86 13895717356.
E-mail address: zhuangjiayuan@163.com (Z. Jiayuan).

0141-1187/$ – see front matter © 2015 Elsevier Ltd. All rights reserved.
http://dx.doi.org/10.1016/j.apor.2015.06.007

Zou applied LS-SVM for parametric identification for underwater vehicles [25].

In the area of parametric identification for ship maneuvering modeling, a matter worthy of attention is that most of the published work is focusing on the development of the SI algorithm, i.e., how to approximate the hydrodynamic derivatives with higher accuracy with the given in–out sample pairs. However, with the sample dataset obtained from experiments or maneuvering simulations, the construction of in–out sample pairs also has great impact on the maneuvering modeling. The commonly used construction method is named Euler sample structure for identification (ESSI) here, because the core concept of this method is based on 1st-order Euler differential method, i.e., discretize the surge acceleration such as $\dot{u}$ as $\dot{u} = (u_{k+1} - u_k)/h$, where h is sample interval [22,23]. Unfortunately, the author's research based on maneuvering simulations suggested that ESSI would be only available when the sample interval is close to the simulation time step[1] [26]. In particular, the most accurate identification results will be gained with ESSI if 1st-order Euler differential method is employed for maneuvering simulation and the simulation time step is equal to the sample interval. Obviously, this is an extremely special and unpractical case which is only available in simulation tests and not realistic for practical application. As usual, 4th-order Runge–Kutta method is more widely adopted as the simulation algorithm. In addition, the simulation time step should be as small as possible to simulate the actual time-continuous system, while the sample interval should be a little bigger for the convenience of experimental measurements.

As a result of such shortcomings of ESSI, a novel sample structure for identification is put forward in this work. We call it integral sample structure for identification (ISSI), because it is based on the integration of the dynamic model. ISSI is also called integral method, while relatively ESSI is also called direct method according to [27,28]. In these two literatures, ISSI is proposed for parametric identification of single degree of freedom (DOF) motion equations for underwater vehicles based on LS method. In essence, there is another sample structure for identification which employed accelerations as the output [29]. However, two fatal problems prohibit this ideology. On one hand, the measurement of the accelerations is an extremely difficult problem. At present, there is no feasible equipment on board for the collection of acceleration data with acceptable accuracy, because accelerometers are highly sensitive to mechanic vibrations [28]. On the other hand, the sampling frequency of the velocity measurement is usually very low, and consequently the calculation of the accelerations based on the differential of the velocities will give impassable results. Therefore, there are few literatures that employ accelerations for the construction of in–out sample pairs.

This paper makes an effort on parametric identification of ship maneuvering motion by using LS-SVM with ISSI and ESSI. The principle of ISSI is deduced at first and it is applied to construct the in–out sample pairs based on Abokowitz model. The sample data used here are obtained from 15/15 zigzag maneuvering simulation of Mariner Class Vessel [30]. The principle of LS-SVM for parametric regression is then introduced. At last, the identification results are compared with their original values, and 25°/25° zigzag test and 30° turning circle test are carried out for validations. The comparisons between the ISSI and ESSI are also implemented.

[1] Simulation time step: the interval used for maneuvering simulation. Sample interval: the interval used for collecting the sample dataset from the experiments or maneuvering simulations.

2. Sample structure for identification

2.1. Euler sample structure for identification

Euler sample structure for identification (ESSI) is the most commonly used approach for the construction of sample pairs. The core concept of this approach is described as follows.

For the dynamic system,

$$\begin{cases} \dot{x} = g(x, \theta, \mu) \\ y = x + \varepsilon \end{cases} \tag{1}$$

where x denotes motion parameter; θ denotes the model parameters; μ is system input; y is the observed system output; ε is measuring error. Here ε is usually considered as zero-mean Gaussian white noise.

Based on Euler 1st-order differential method, $\dot{x} = x_{k+1} - x_k/h$. Then Eq. (1) can be rewritten as,

$$\begin{cases} x_{k+1} = x_k + hg(x_k, \theta, \mu_k) \\ y_{k+1} = x_{k+1} + \varepsilon_{k+1} \end{cases} \tag{2}$$

where h is sample interval.

The hydrodynamic derivatives in the mathematical model of ship maneuvering motion are considered as constant values, and the mathematical model is linear function about the hydrodynamic derivatives. Consequently, $g(x, \theta, \mu)$ can be rewritten as,

$$g(x, \theta, \mu) = P(x, \mu)\left[\theta_1, \theta_2, \ldots, \theta_m\right]^{\mathrm{T}} \tag{3}$$

where $P(x, \mu) = [P_1(x, \mu), P_2(x, \mu), \ldots, P_m(x, \mu)]$, m is the number of the identified parameters.

If there are totally $n+1$ sample data, the problem of system identification turns to the solution of n-dimension linear equations. Replacing the state variable x_i with its observation y_i, Eq. (2) gives,

$$\begin{bmatrix} x_1 & P_1(x_1, \mu_1) & P_2()x_1, \mu_1 & \cdots & P_m(x_1, \mu_1) \\ x_2 & P_1(x_2, \mu_2) & P_2(x_2, \mu_2) & \cdots & P_m(x_2, \mu_2) \\ \vdots & \vdots & \vdots & \ddots & \vdots \\ x_n & P_1(x_n, \mu_n) & P_2(x_n, \mu_n) & \cdots & P_m(x_n, \mu_n) \end{bmatrix} \begin{bmatrix} 1 \\ \theta_1 \\ \vdots \\ \theta_m \end{bmatrix} + \begin{bmatrix} \varepsilon_1 \\ \varepsilon_2 \\ \vdots \\ \varepsilon_n \end{bmatrix} = \begin{bmatrix} x_2 \\ x_3 \\ \vdots \\ x_{n+1} \end{bmatrix} \tag{4}$$

Rewriting the above equations with uniform and compact matrix form,

$$\mathcal{Y} = \mathcal{X}\theta + \varepsilon \tag{5}$$

where $\mathcal{X}$ are the input samples, and $\mathcal{Y}$ are the output samples. It is easy to find that Eq. (5) is the commonly used standard form for SI. The parameters θ can be obtained by using SI algorithm.

Based on the above analysis, the in–out sample pairs for ESSI can be confirmed as,

$$\left\{ \begin{array}{l} \text{input} : \left\{x_k, P_1(x_k, \mu_k), P_2(x_k, \mu_k), \ldots, P_m(x_k, \mu_k)\right\} \\ \text{output} : \left\{x_{k+1}\right\} \end{array} \right\}$$

2.2. Integral sample structure for identification

The proposed sample structure for identification is deduced from the integration of the dynamic model, and is accordingly called integral sample structure for identification (ISSI). The formation of ISSI is already deduced in [27], however new manner is proposed for easier understanding in this paper. The core concept of this method is described as follows.

For the same dynamic model as described in Eq. (1), integrating both the sides of Eq. (1) yields,

$$x_k = \int_0^{t_k} g(x, \theta, \mu)dt, \qquad x_{k+1} = \int_0^{t_{k+1}} g(x, \theta, \mu)dt \tag{6}$$

where k is time step. Subtracting x_k from x_{k+1} gives,

$$x_{k+1} - x_k = \int_{t_k}^{t_{k+1}} g(x, \theta, \mu)dt \tag{7}$$

Since

$$y_{k+1} = x_{k+1} + \varepsilon_{k+1}, \qquad y_k = x_k + \varepsilon_k \tag{8}$$

Subtracting y_k from y_{k+1} gives,

$$y_{k+1} - y_k = \int_{t_k}^{t_{k+1}} g(x, \theta, \mu)dt + (\varepsilon_{k+1} - \varepsilon_k) \tag{9}$$

Obviously, if the statistical characteristic of ε is zero-mean Gaussian white noise, $[\varepsilon_2 - \varepsilon_1, \varepsilon_3 - \varepsilon_2, \ldots, \varepsilon_{k+1} - \varepsilon_k, \ldots]$ can also be considered as zero-mean Gaussian white noise.

If the sample number is totally $n+1$, separating the constant variables from $g(x, \theta, \mu)$ based on Eq. (3), and replacing the observation value y_i with its system value x_i, the problem of SI is transferred to the solution of the following n-dimension linear equations,

$$\begin{bmatrix} x_1 & \int_{t_1}^{t_2} P_1(x,\mu)dt & \int_{t_1}^{t_2} P_2(x,\mu)dt & \cdots & \int_{t_1}^{t_2} P_m(x,\mu)dt \\ x_2 & \int_{t_2}^{t_3} P_1(x,\mu)dt & \int_{t_2}^{t_3} P_2(x,\mu)dt & \cdots & \int_{t_2}^{t_3} P_m(x,\mu)dt \\ \vdots & \vdots & \vdots & \ddots & \vdots \\ x_n & \int_{t_n}^{t_{n+1}} P_1(x,\mu)dt & \int_{t_n}^{t_{n+1}} P_2(x,\mu)dt & \cdots & \int_{t_n}^{t_{n+1}} P_m(x,\mu)dt \end{bmatrix} \begin{bmatrix} 1 \\ \theta_1 \\ \theta_2 \\ \vdots \\ \theta_m \end{bmatrix} + \begin{bmatrix} \varepsilon_2 - \varepsilon_1 \\ \varepsilon_3 - \varepsilon_2 \\ \vdots \\ \varepsilon_{n+1} - \varepsilon_n \end{bmatrix} = \begin{bmatrix} x_2 \\ x_3 \\ \vdots \\ x_{n+1} \end{bmatrix} \tag{10}$$

The above equations are the standard format for SI, and the in–out sample pairs for ISSI can be obtained,

$$\left\{ \begin{array}{l} \text{input}: \left\{ x_k, \int_{t_k}^{t_{k+1}} P_1(x,\mu)dt, \int_{t_k}^{t_{k+1}} P_2(x,\mu)dt, \ldots, \int_{t_k}^{t_{k+1}} P_m(x,\mu) \right\} \\ \text{output}: \{x_{k+1}\} \end{array} \right\}$$

It can be seen that the core problem for ISSI is the solution of the integral problem, i.e., the calculation of $\int_{t_k}^{t_{k+1}} P_i(x, \mu)dt$, and it is in close correlation with the precision of parametric identification. If 1st-order Euler differential method is used for the solution of the integral problem as shown in Eq. (11), ISSI is equal to ESSI at this time [22,23].

$$\int_{t_k}^{t_{k+1}} P_i(x, \mu)dt = P_i(x_k, \mu_k)(t_{k+1} - t_k) \tag{11}$$

Obviously, there are many other algorithms for the solution of the integration. For simplification, herein trapezoid method is employed for calculating the integration and the formulation is shown in Eq. (12).

$$\int_{t_k}^{t_{k+1}} P_i(x, \mu)dt = \frac{(t_{k+1} - t_k)\,[P_i(x_{k+1}, \mu_{k+1}) + P_i(x_k, \mu_k)]}{2} \tag{12}$$

3. Mathematical model of ship maneuvering motion

To describe the motion characteristics of a ship, two coordinate systems are usually adopted, i.e., the global or earth-fixed coordinate system *GXYZ* and the local or body-fixed coordinate system $OX_0Y_0Z_0$, as shown in Fig. 1. The motion parameters u, v, w, p, q and r represent the kinematic velocities in surge, sway, heave, roll, pitch and roll motions, respectively.

Generally, 6-DOF motion equations should be built to characterize the ship motion, but the reduced 4-DOF motion equations, i.e., surge, sway, roll and yaw, are usually considered because the amplitudes of heave and pitch are too small to be ignored. For some high speed ships, the ships have low metacentric height or need high comfort requirements, e.g., the warships, container vessels, and passenger ships, the 4-DOF motion equations must be considered. However, for other ordinary ships, the roll motion is usually not taken into consideration, and the 4-DOF motion equations can be further simplified to 3-DOF, i.e., surge, sway and yaw.

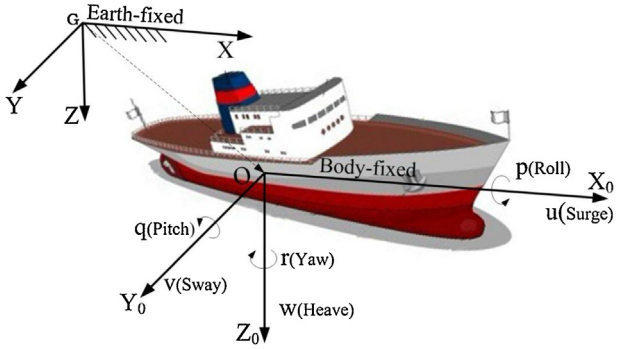

Fig. 1. Global and local coordinate systems for ship.

Herein, 3-DOF Abkowitz model is adopted for consideration. The original Abkowitz model includes 65 hydrodynamic derivatives. According to Chislett et al.'s experimental results, the hydrodynamic derivatives can be reduced to 45 [31]. The simplified Abkowitz model can be written in a uniform and compact matrix form as follows [30],

$$\begin{bmatrix} m' - X'_{\dot{u}} & 0 & 0 \\ 0 & m' - Y'_{\dot{v}} & m'x'_G - Y'_{\dot{r}} \\ 0 & m'x'_G - N'_{\dot{v}} & I'_Z - N'_{\dot{r}} \end{bmatrix} \begin{bmatrix} \Delta\dot{u}' \\ \Delta\dot{v}' \\ \Delta\dot{r}' \end{bmatrix} = \begin{bmatrix} \Delta f'_1 \\ \Delta f'_2 \\ \Delta f'_3 \end{bmatrix} \tag{13}$$

where the parameter with a superscript '" denotes that it is non-dimensional. Under this regulation, m is the mass of the ship; I_z is the inertia moment about z-axis; x_G is the longitudinal coordinate of the mass center in body-fixed coordinates; $\Delta\dot{u}$, $\Delta\dot{v}$ and $\Delta\dot{r}$ denote the acceleration or angler acceleration in surge, sway and yaw motions, respectively; $X_{\dot{u}}$, $Y_{\dot{v}}$ and $N_{\dot{r}}$ etc. are inertia hydrodynamics; Δf_1, Δf_2 and Δf_3 are force/moment in surge, sway and yaw motions, respectively, and the expanded description of them are given as follows,

$$\begin{aligned} \Delta f'_1 &= X'_u\Delta u' + X'_{uu}\Delta u'^2 + X'_{uuu}\Delta u'^3 + X'_{vv}\Delta v'^2 + X'_{rr}\Delta r'^2 + X'_{\delta\delta}\Delta\delta'^2 \\ &\quad + X'_{\delta\delta u}\Delta\delta'^2\Delta u' + X'_{vr}\Delta v'\Delta r' + X'_{v\delta}\Delta v'\Delta\delta' + X'_{v\delta u}\Delta v'\Delta\delta'\Delta u' \end{aligned}$$

$$\begin{aligned} \Delta f'_2 &= Y'_{0u}\Delta u' + Y'_{0uu}\Delta u'^2 + Y'_v\Delta v' + Y'_r\Delta r' + Y'_\delta\Delta\delta' + Y'_{vvv}\Delta v'^3 + Y'_{\delta\delta\delta}\Delta\delta'^3 \\ &\quad + Y'_{vvr}\Delta v'^2\Delta r' + Y'_{vv\delta}\Delta v'^2\Delta\delta' + Y'_{v\delta\delta}\Delta v'\Delta\delta'^2 + Y'_{\delta u}\Delta\delta'\Delta u' \\ &\quad + Y'_{vu}\Delta v'\Delta u' + Y'_{ru}\Delta r'\Delta u' + Y'_{\delta uu}\Delta\delta'\Delta u'^2 + Y'_0 \end{aligned}$$

$$\begin{aligned}\Delta f_3' &= N_{0u}'\Delta u' + N_{0uu}'\Delta u'^2 + N_v'\Delta v' + N_r'\Delta r' + N_\delta'\Delta\delta' + N_{vvv}'\Delta v'^3 \\ &+N_{\delta\delta\delta}'\Delta\delta'^3 + N_{vvr}'\Delta v'^2\Delta r' + N_{vv\delta}'\Delta v'^2\Delta\delta' + N_{v\delta\delta}'\Delta v'\Delta\delta'^2 \\ &+N_{\delta u}'\Delta\delta'\Delta u' + N_{vu}'\Delta v'\Delta u' + N_{ru}'\Delta r'\Delta u' + N_{\delta uu}'\Delta\delta'\Delta u'^2 + N_0'\end{aligned}$$

where X_u', Y_{0u}' and N_{0u}' etc. are non-dimensional hydrodynamic derivatives; $\Delta u'$, $\Delta v'$ and $\Delta r'$ denote the non-dimensional surge velocity, sway velocity and yaw rate, respectively; $\Delta\delta'$ is non-dimensional rudder angle. With the exception of hydrodynamic derivatives, the transformations between the dimensional and non-dimensional forms for the above parameters are arranged as follows,

$$m' = \frac{m}{1/2\rho L^3}, x_G' = \frac{x_G}{L}, I_z' = \frac{I_z}{1/2\rho L^5}, \Delta\dot{u}' = \frac{\Delta\dot{u}}{U^2/L}, \Delta\dot{v}' = \frac{\Delta\dot{v}}{U^2/L},$$
$$\Delta\dot{r}' = \frac{\Delta\dot{r}}{U^2/L^2}, \Delta u' = \frac{\Delta u}{U}, \Delta v' = \frac{\Delta v}{U}, \Delta r' = \frac{\Delta r}{U}, \Delta\delta' = \Delta\delta$$

where L is the ship length; ρ is the density of water; U is the total velocity. With the straight forward motion with constant speed u_0 as the initial condition, we have the variables $u = u_0 + \Delta u$, $v = \Delta v$, $r = \Delta r$ and $\delta = \Delta\delta$, and the total velocity is given by $U = \sqrt{(u_0+\Delta u)^2 + \Delta v^2}$.

For the convenience of computer simulation and parametric identification, Eq. (13) is transformed to the following non-dimensional state-space model,

$$\begin{cases}\Delta\dot{u}' = \Delta f_1'/(m' - X_{\dot{u}}') \\ \Delta\dot{v}' = \left[(I_Z' - N_{\dot{r}}')\Delta f_2' - (m'x_G' - Y_{\dot{r}}')\Delta f_3'\right]/S \\ \Delta\dot{r}' = \left[(m' - Y_{\dot{v}}')\Delta f_3' - (m'x_G' - N_{\dot{v}}')\Delta f_2'\right]/S\end{cases} \quad (14)$$

where $S = (I_z' - N_{\dot{r}}')(m' - Y_{\dot{v}}') - (m'x_G' - Y_{\dot{r}}')(m'x_G' - N_{\dot{v}}')$.

Furthermore, the non-dimensional parameters except hydrodynamic derivatives and physical parameters are transformed to dimensional format for Eq. (14), and the incomplete dimensional form of the mathematical model is shown as follows,

$$\begin{aligned}\Delta\dot{u} = &\frac{1}{L(m' - X_{\dot{u}}')}\left[X_u'\Delta uU + X_{uu}'\Delta u^2 + X_{uuu}'\Delta u^3/U + X_{vv}'\Delta v^2 + X_{rr}'\Delta r^2L^2\right. \\ &\left.+X_{\delta\delta}'\Delta\delta^2U^2 + X_{\delta\delta u}'\Delta\delta^2\Delta uU + X_{vr}'\Delta v\Delta rL + X_{v\delta}'\Delta v\Delta\delta U + X_{v\delta u}'\Delta v\Delta\delta\Delta u\right]\end{aligned} \quad (15)$$

$$\begin{aligned}\Delta\dot{v} = &\frac{I_Z' - N_{\dot{r}}'}{SL}\left[Y_0'U^2 + Y_{0u}'\Delta uU + Y_{0uu}'\Delta u^2 + Y_v'\Delta vU + Y_r'\Delta rUL + Y_\delta'\Delta\delta U^2\right. \\ &+Y_{vvv}'\Delta v^3/U + Y_{\delta\delta\delta}'\Delta\delta^3U^2 + Y_{vvr}'\Delta v^2\Delta rL/U + Y_{vv\delta}'\Delta v^2\Delta\delta + Y_{v\delta\delta}'\Delta v\Delta\delta^2U \\ &\left.+Y_{\delta u}'\Delta\delta\Delta uU + Y_{vu}'\Delta v\Delta u + Y_{ru}'\Delta r\Delta uL + Y_{\delta uu}'\Delta\delta\Delta u^2\right] - \frac{m'x_G' - Y_{\dot{r}}'}{SL}\left[N_0'U^2\right. \\ &+N_{0u}'\Delta uU + N_{0uu}'\Delta u^2 + N_v'\Delta vU + N_r'\Delta rUL + N_\delta'\Delta\delta U^2 + N_{vvv}'\Delta v^3/U \\ &+N_{\delta\delta\delta}'\Delta\delta^3U^2 + N_{vvr}'\Delta v^2\Delta rL/U + N_{vv\delta}'\Delta v^2\Delta\delta + N_{v\delta\delta}'\Delta v\Delta\delta^2U + N_{\delta u}'\Delta\delta\Delta uU \\ &\left.+N_{vu}'\Delta v\Delta u + N_{ru}'\Delta r\Delta uL + N_{\delta uu}'\Delta\delta\Delta u^2\right]\end{aligned} \quad (16)$$

$$\begin{aligned}\Delta\dot{r} = &-\frac{m'x_G' - N_{\dot{v}}'}{SL^2}\left[Y_0'U^2 + Y_{0u}'\Delta uU + Y_{0uu}'\Delta u^2 + Y_v'\Delta vU + Y_r'\Delta rUL + Y_\delta'\Delta\delta U^2\right. \\ &+Y_{vvv}'\Delta v^3/U + Y_{\delta\delta\delta}'\Delta\delta^3U^2 + Y_{vvr}'\Delta v^2\Delta rL/U + Y_{vv\delta}'\Delta v^2\Delta\delta + Y_{v\delta\delta}'\Delta v\Delta\delta^2U \\ &\left.+Y_{\delta u}'\Delta\delta\Delta uU + Y_{vu}'\Delta v\Delta u + Y_{ru}'\Delta r\Delta uL + Y_{\delta uu}'\Delta\delta\Delta u^2\right] + \frac{m' - Y_{\dot{v}}'}{SL^2}\left[N_0'U^2 + \right. \\ &+N_{0u}'\Delta uU + N_{0uu}'\Delta u^2 + N_v'\Delta vU + N_r'\Delta rUL + N_\delta'\Delta\delta U^2 + N_{vvv}'\Delta v^3/U \\ &+N_{\delta\delta\delta}'\Delta\delta^3U^2 + N_{vvr}'\Delta v^2\Delta rL/U + N_{vv\delta}'\Delta v^2\Delta\delta + N_{v\delta\delta}'\Delta v\Delta\delta^2U + N_{\delta u}'\Delta\delta\Delta uU \\ &\left.+N_{vu}'\Delta v\Delta u + N_{ru}'\Delta r\Delta uL + N_{\delta uu}'\Delta\delta\Delta u^2\right]\end{aligned} \quad (17)$$

With the conception of variable separation technique as shown in Eq. (3), the terms in the right hands of Eqs. (15)–(17) can be divided into two sections. One section is comprised of constant numerical values. The other section contains motion variables which are used for the construction of input samples. Based on ISSI and Eqs. (15)–(17), the input samples can be constructed as follows,

$$\begin{aligned}X = &\left[\Delta u_k, \int_{t_k}^{t_{k+1}}\Delta uUdt, \int_{t_k}^{t_{k+1}}\Delta u^2dt, \int_{t_k}^{t_{k+1}}\frac{\Delta u^3}{U}dt, \int_{t_k}^{t_{k+1}}\Delta v^2dt, \int_{t_k}^{t_{k+1}}\Delta r^2dt, \int_{t_k}^{t_{k+1}}\Delta\delta^2U^2dt,\right. \\ &\left.\int_{t_k}^{t_{k+1}}\Delta\delta^2\Delta uUdt, \int_{t_k}^{t_{k+1}}\Delta v\Delta rdt, \int_{t_k}^{t_{k+1}}\Delta v\Delta\delta Udt, \int_{t_k}^{t_{k+1}}\Delta v\Delta\delta\Delta udt\right]^T_{11\times1}\end{aligned}$$

$$\begin{aligned}Y = &\left[\Delta v_k, \int_{t_k}^{t_{k+1}}U^2dt, \int_{t_k}^{t_{k+1}}\Delta uUdt, \int_{t_k}^{t_{k+1}}\Delta u^2dt, \int_{t_k}^{t_{k+1}}\Delta vUdt, \int_{t_k}^{t_{k+1}}\Delta rUdt, \int_{t_k}^{t_{k+1}}\Delta\delta U^2dt,\right. \\ &\int_{t_k}^{t_{k+1}}\frac{\Delta v^3}{U}dt, \int_{t_k}^{t_{k+1}}\Delta\delta^3U^2dt, \int_{t_k}^{t_{k+1}}\frac{\Delta v^2\Delta r}{U}dt, \int_{t_k}^{t_{k+1}}\Delta v^2\Delta\delta dt, \int_{t_k}^{t_{k+1}}\Delta v\Delta\delta^2dt, \\ &\left.\int_{t_k}^{t_{k+1}}\Delta\delta\Delta uUdt, \int_{t_k}^{t_{k+1}}\Delta v\Delta udt, \int_{t_k}^{t_{k+1}}\Delta r\Delta udt, \int_{t_k}^{t_{k+1}}\Delta\delta\Delta u^2dt\right]^T_{16\times1}\end{aligned}$$

$$\begin{aligned}Z = &\left[\Delta r_k, \int_{t_k}^{t_{k+1}}U^2dt, \int_{t_k}^{t_{k+1}}\Delta uUdt, \int_{t_k}^{t_{k+1}}\Delta u^2dt, \int_{t_k}^{t_{k+1}}\Delta vUdt, \int_{t_k}^{t_{k+1}}\Delta rUdt, \int_{t_k}^{t_{k+1}}\Delta\delta U^2dt,\right. \\ &\int_{t_k}^{t_{k+1}}\frac{\Delta v^3}{U}dt, \int_{t_k}^{t_{k+1}}\Delta\delta^3U^2dt, \int_{t_k}^{t_{k+1}}\frac{\Delta v^2\Delta r}{U}dt, \int_{t_k}^{t_{k+1}}\Delta v^2\Delta\delta dt, \int_{t_k}^{t_{k+1}}\Delta v\Delta\delta^2dt, \\ &\left.\int_{t_k}^{t_{k+1}}\Delta\delta\Delta uUdt, \int_{t_k}^{t_{k+1}}\Delta v\Delta udt, \int_{t_k}^{t_{k+1}}\Delta r\Delta udt, \int_{t_k}^{t_{k+1}}\Delta\delta\Delta u^2dt\right]^T_{16\times1}\end{aligned}$$

where X, Y and Z denote the input samples of surge, sway and yaw motions, respectively. The integral problem in the input samples

Table 1
Physical parameters of Mariner Class Vessel.

Length overall L_{aa} (m)	171.80
Length between perpendiculars L_{pp} (m)	160.93
Maximum beam B (m)	23.17
Design draft T (m)	8.23
Design displacement ∇ (m^3)	18,541
Design speed u_0 (knots)	15

can be solved by using trapezoid method. Taking $\int_{t_k}^{t_{k+1}} \Delta u U dt$ for example, the calculation of the integration is,

$$\int_{t_k}^{t_{k+1}} \Delta u U dt = \frac{(t_{k+1}-t_k)(\Delta u_k U_k + \Delta u_{k+1} U_{k+1})}{2} = \frac{h(\Delta u_k U_k + \Delta u_{k+1} U_{k+1})}{2} \tag{18}$$

where $h = t_{k+1} - t_k$ is the sample interval.

If the constant numerical values in Eqs. (15)–(17) are represented by the following simple symbols,

$$\text{Surge}: \quad A = [a_0, a_1, a_2, \ldots, a_{10}]$$

$$\text{Sway}: \quad B = [b_0, b_1, b_2, \ldots, b_{15}]$$

$$\text{Yaw}: \quad C = [c_0, c_1, c_2, \ldots, c_{15}]$$

The output samples can be simply described as,

$$\Delta u_{k+1} = AX$$

$$\Delta v_{k+1} = BY$$

$$\Delta r_{k+1} = CZ$$

Once the unknown vectors A, B and C are solved, each hydrodynamic derivative can be gained. The derivatives in surge motion can be straightforwardly gained from A. The operation is as follows,

$$X'_i = \frac{2a_i L(m' - X'_{\dot{u}})}{h} \tag{19}$$

Here, the parameters X'_i must be divided by L^2 when $i = 5$ and divided by L when $i = 8$, respectively. The derivatives in sway and yaw motions can be indirectly gained by solving the following two-dimensional system of equations,

$$\frac{h}{2}\begin{bmatrix} \frac{I'_Z - N'_{\dot{r}}}{SL} & -\frac{m'x'_G - Y'_{\dot{r}}}{SL} \\ -\frac{m'x'_G - N_{\dot{v}}}{SL^2} & \frac{m' - Y'_{\dot{v}}}{SL^2} \end{bmatrix} \begin{bmatrix} Y_i \\ N_i \end{bmatrix} = \begin{bmatrix} b_i \\ c_i \end{bmatrix} \tag{20}$$

Here, the parameters Y'_i and N'_i must be divided by L when $i = 5,9$ and 14. It is worth noting that a_0, b_0 and c_0 are dummy terms, i.e., the identification of these three terms is of no significance.

4. Numerical results

In this work, Mariner Class Vessel is used for maneuvering simulation to validate the proposed method. The hydrodynamic and aerodynamics laboratory in Lyngby, Denmark has performed both planar motion mechanism (PMM) tests and full-scale steering and maneuvering prediction for this vessel. The main data and dimensions of this vessel can be shown in Table 1. The hydrodynamic derivatives are obtained from PMM tests [31].

Generally, there are three important facets for parametric identification with simulated data, i.e., collection of data samples, construction of sample structure, and choice of identification algorithm.

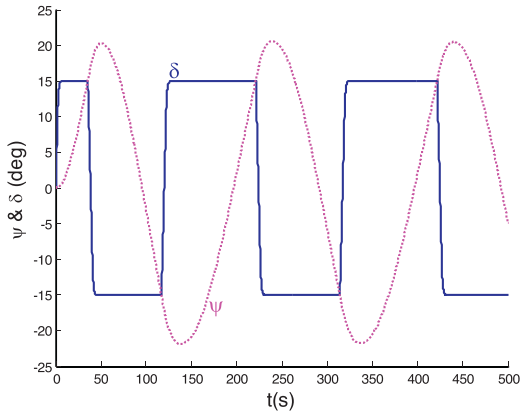

Fig. 2. Time histories of yaw angle and rudder angle in 15°/15° zigzag test.

The sample data prepared for parametric identification must be sufficient and reflect the real characteristics of the dynamic model. To achieve this target, 15°/15° zigzag test is conducted by using 4th-order Runge–Kutta method, where the simulation time step is set as $\Delta t = 0.1$ s and the simulation time is set as 500 s. Besides, the initial surge velocity is set as $U_0 = 7.7175$ m/s.

The mathematical model of steering gear for the rudder is defined as,

$$\dot{\delta} = \begin{cases} (\delta^* - \delta)/T_E; & \left|\delta^* - \delta\right| \le T_E \left|\dot{\delta}_{\max}\right| \\ sign(\delta^* - \delta)\left|\dot{\delta}_{\max}\right|; & \left|\delta^* - \delta\right| > T_E \left|\dot{\delta}_{\max}\right| \end{cases} \tag{21}$$

where δ is the actuator angle, $\delta^*$is the command angle, T_E is the sample interval, $\left|\dot{\delta}_{\max}\right| = 5^\circ/s$ is the maximum fin turning rate.

Under this condition, a fully developed zigzag maneuver is gained as shown in Fig. 2. The obtained sample number is 5001 in total.

Based on integral sample structure for identification, the in–out sample pairs can be gained as described in Section 3. The sample interval is set as 0.5 s, and 1000 sample pairs can be gained. Thus, the last important facet is the identification algorithm, which should be as accurate as possible. Herein LS-SVM is employed for parametric identification.

LS-SVM shows good performance in solving classification and regression problems and has been widely used in pattern recognition, model regression, optimal control and so on [32,33]. LS-SVM is a special type of SVM. It chooses the square cost function, which leads to the loss of sparse solution, i.e., all the input samples are support vectors. However, LS-SVM transforms the solution of quadratic optimization problem to a linear system of equations, which greatly simplifies the solution problem. The resolution flow of LS-SVM is given as follows.

With the given training data set (x,y), the feature space representation of LS-SVM is given by

$$y(x) = w^T \varphi(x) + b (x \in \mathbb{R}^m, y \in \mathbb{R}) \tag{22}$$

where w is a vector in the so-called high dimensional feature space, $\varphi(\cdot)$ is the mapping function that maps the input data to a high dimensional feature space. b is a bias for the regression model. The optimization problem is formulated as the following optimization problem:

$$\min_{w,e} J(w, 2) = \frac{1}{2} w^T w + \frac{1}{2} C \sum_{i=1}^{n} e_i^2 \tag{23}$$

subject to the following constraints

$$y_i = w^T \varphi(x_i) + b + e_i \qquad i = 1, \ldots, n \tag{24}$$

where C is rule factor, e is regression error.

Lagrangian function is defined for target function and constraint conditions,

$$L(w, b, e, \alpha) = J(w, e) - \sum_{i=1}^{n} \alpha_i \left\{ w^T \varphi(x_i) + b + e_i - y_i \right\} \tag{25}$$

where α_i is lagrangian multiplier. Partial derivatives of L with respect to w, b, e, α, we have

$$\begin{cases} \dfrac{\partial L}{\partial w} = 0 \rightarrow w = \sum_{i=1}^{n} \alpha_i \varphi(x_i) \\ \dfrac{\partial L}{\partial w} = 0 \rightarrow \sum_{i=1}^{n} \alpha_i = 0 \\ \dfrac{\partial L}{\partial w} = 0 \rightarrow \alpha_i = Ce_i \\ \dfrac{\partial L}{\partial w} = 0 \rightarrow w^T \varphi(x_i) + b + e_i - y_i = 0 \end{cases} \tag{26}$$

Substitute the first and third formulas to the forth and subject to the second, gives

$$\begin{bmatrix} 0 & \vec{1} \\ \vec{1}^T & \Omega + C^{-1} I \end{bmatrix} \begin{bmatrix} b \\ \alpha \end{bmatrix} = \begin{bmatrix} 0 \\ y \end{bmatrix} \tag{27}$$

where $\rightarrow 1 = [1, 1, \ldots, 1]$, $0 = [0, \ldots, 0]^{\mathrm{T}}$, $y = [y_1, y_2, \ldots, y_n]^{\mathrm{T}}$, n is the number of the data sample; $\alpha = [\alpha_1, \alpha_2, \ldots, \alpha_n]$ are Lagrange multipliers; C is the rule factor, which can be chosen by experience or parameter optimization; $\Omega_{ij} = \varphi(x_i)^{\mathbf{T}} \varphi(x_j) = K(x_i, x_j)$, $(i, j = 1, 2, \ldots, n)$, and $K(x_i, x_j)$ is the kernel function.

The solution of LS-SVM can be converted to a linear system of equations via a series of transformation. The set of equations of $n+1$ dimensions are shown as follows [33],

$$\begin{bmatrix} 0 & \vec{1} \\ \vec{1}^{\mathrm{T}} & \Omega + C^{-1} I \end{bmatrix} \begin{bmatrix} b \\ \alpha \end{bmatrix} = \begin{bmatrix} \vec{0} \\ y \end{bmatrix} \tag{28}$$

where $\rightarrow 1 = [1, 1, \ldots, 1]$; $y = [y_1, y_2, \ldots, y_n]^{\mathbf{T}}$, n is the number of the data sample; $\alpha = [\alpha_1, \alpha_2, \ldots, \alpha_n]$ are Lagrange multipliers; C is the rule factor, which can be chosen by experience or parameter optimization; $\Omega_{ij} = \varphi(x_i)^{\mathbf{T}} \varphi(x_j) = K(x_i, x_j)$, $(i, j = 1, 2, \ldots, n)$, and $K(x_i, x_j)$ is the kernel function.

Once Eq. (28) is solved, the regression model can be gained,

$$y(x) = \sum_{i=1}^{n} \alpha_i K(x_i, x) + b \tag{29}$$

For the problem of parametric identification, linear kernel function is usually adopted, i.e., $K(x, x') = (x \cdot x')$. The identified parameters can be regressed by using linear kernel based LS-SVM, and the regression model is,

$$\theta = \sum_{i=1}^{n} \alpha_i x_i \tag{30}$$

where θ denotes the identified parameters. Furthermore, the rule factor is not very sensitive to the regression results in a large extent if linear kernel function is selected. It can be set as a large numerical value by the users' experience.

Based on parameter's identifiability theory, the inertial hydrodynamic derivatives are not concerned for parametric identification [34]. They can be approximated with other approaches such as estimation with empirical formula. With the sample dataset obtained by 15°/15° zigzag test, the hydrodynamic derivatives in Abokowitz model are identified with the integral sample structure based on LS-SVM. The rule factor in LS-SVM is set as 4×10^6, 6×10^8 and 6×10^8 for surge, sway and yaw motions, respectively. To diminish the effect of parameter drift, additional excitation method is put to use. Three random number series are added into the input and output samples according to [22,23]. Along with the change of the random number series, the identified hydrodynamic derivatives will vary in a very small extent, which is convenient for the selection of the random number series.

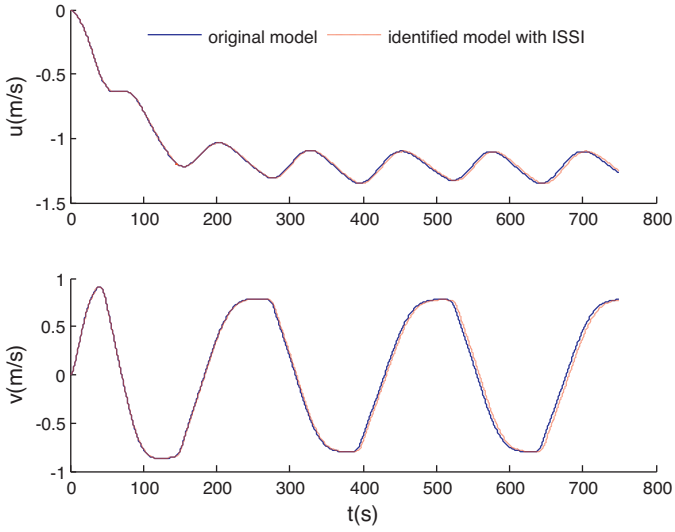

Fig. 3. Time histories of surge and sway velocities of 25°/25° zigzag test.

The identification results are shown in Tables 2–4. It has to be pointed out that the numerical values of the identified results and relative errors are all rounded. The relative errors between the original and identified hydrodynamic derivatives demonstrate that most of the identified coefficients are in good agreement with their original numerical values except a few terms. The dissatisfactory coefficients include Y'_{0uu}, $Y'_{v\delta\delta}$ N'_{0uu} and $N'_{v\delta\delta}$. In fact, these dissatisfactory coefficients are those who have little impact on the maneuvering model, i.e., some changes or eliminations of these coefficients will not greatly affect the maneuvering simulation or prediction. The reasonable explanation for these big relative errors can attributes to sensitivity analysis of hydrodynamic derivatives. The sensitivity values of these dissatisfactory coefficients are all very small by referring to the research of Xu et al. [35], which indicates that they are not significant for the maneuvering model, while small sensitivity values are in corresponding with bad identification results [25,36].

To further validate the identified hydrodynamic derivatives, 25°/25° zigzag test and 30° turning circle test are carried out for maneuvering prediction by using the original and identified hydrodynamic derivatives, respectively. The simulation results are shown in Figs. 3–6. The comparison between the original and identified models shows the validation of the identified hydrodynamic derivatives, as well as the effectiveness of the proposed ISSI.

In addition, to compare the validation of the proposed ISSI with the commonly used ESSI, the hydrodynamic derivatives are identified again based on ESSI with the same identification algorithm and dataset. The construction of the in–out sample pairs with ESSI can be referred to [22,23]. Herein the sample interval is also set as 0.5 s, and keeps the rule factors unchanged. Besides, random number series are also used as the additional excitation to decrease the parameter drift. The identification results are shown in Tables 5–7. The numerical values of the identified results and relative errors are also rounded. These tables suggest that most of the identification results are away from their original values except several

Table 2
Identified hydrodynamic derivatives of surge motion with ISSI ($\times 10^{-5}$).

Surge	X'_u	X'_{uu}	X'_{uuu}	X'_{vv}	X'_{rr}	$X'_{\delta\delta}$	$X'_{\delta\delta u}$	X'_{vr}	$X'_{v\delta}$	$X'_{v\delta u}$
Original	−184	−110	−215	−899	18	−95	−190	798	93	93
Identified	−184	−111	−213	−896	18	−95	−188	801	93	95
Error (%)	0	1	1	0	2	0	1	0	0	3

Table 3
Identified hydrodynamic derivatives of sway motion with ISSI ($\times 10^{-5}$).

Sway	Y'_0	Y'_{0u}	Y'_{0uu}	Y'_v	Y'_r	Y'_δ	Y'_{vvv}	$Y'_{\delta\delta\delta}$
Original	−4	−8	−4	−1160	−499	278	−8078	−90
Identified	−4	−8	−7	−1158	−498	279	−7867	−100
Error (%)	1	6	75	0	0	0	3	11

Sway	Y'_{vvr}	$Y'_{vv\delta}$	$Y'_{v\delta\delta}$	$Y'_{\delta u}$	N'_0	N'_{0u}	N'_{0uu}
Original	15,356	1190	−4	556	−1160	−499	278
Identified	15,470	1212	−10	559	−1153	−496	296
Error (%)	1	2	156	1	1	1	7

Table 4
Identified hydrodynamic derivatives of yaw motion with ISSI ($\times 10^{-5}$).

Sway	N'_0	N'_{0u}	N'_{0uu}	N'_v	N'_r	N'_δ	N'_{vvv}	$N'_{\delta\delta\delta}$
Original	3	6	3	−264	−166	−139	1636	45
Identified	3	6	2	−265	−166	−140	1551	50
Error (%)	0	1	24	0	0	0	5	12

Sway	N'_{vvr}	$N'_{vv\delta}$	X'_u	X'_{uu}	X'_{uuu}	X'_{vv}	X'_{rr}
Original	−5483	−489	13	−278	−264	−166	−139
Identified	−5525	−492	−11	−278	−266	−166	−139
Error (%)	1	1	14	0	0	0	0

Table 5
Identified hydrodynamic derivatives of surge motion with ESSI ($\times 10^{-5}$).

Surge	X'_u	X'_{uu}	X'_{uuu}	X'_{vv}	X'_{rr}	$X'_{\delta\delta}$	$X'_{\delta\delta u}$	X'_{vr}	$X'_{v\delta}$	$X'_{v\delta u}$
Original	−184	−110	−215	−899	18	−95	−190	798	93	93
Identified	−188	−208	−686	−821	15	−96	−201	816	90	83
Error (%)	2	89	219	9	16	1	6	2	4	11

Table 6
Identified hydrodynamic derivatives of sway motion with ESSI ($\times 10^{-5}$).

Sway	Y'_0	Y'_{0u}	Y'_{0uu}	Y'_v	Y'_r	Y'_δ	Y'_{vvv}	$Y'_{\delta\delta\delta}$
Original	−4	−8	−4	−1160	−499	278	−8078	−90
Identified	−3	45	358	−1181	−470	288	−10,655	−123
Error (%)	36	664	9038	2	6	3	32	37

Sway	Y'_{vvr}	$Y'_{vv\delta}$	$Y'_{v\delta\delta}$	$Y'_{\delta u}$	N'_0	N'_{0u}	N'_{0uu}
Original	15,356	1190	−4	556	−1160	−499	278
Identified	13,576	−142	875	342	−1422	−588	−1035
Error (%)	12	112	21,978	38	23	18	472

hydrodynamic derivatives including X'_u, X'_{vv}, X'_{vr}, X'_{rr}, $X'_{\delta\delta}$, $X'_{v\delta u}$, $X'_{v\delta}$, $X'_{\delta\delta u}$, X'_{vv}, Y'_r, Y'_{vvr}, Y'_v, Y'_δ, N'_r, N'_v and N'_δ. The author's research in [35] indicates that these coefficients with small relative errors have relatively larger sensitivity values than those with relatively big errors. In other words, the coefficients such as X'_u and Y'_r play a dominant role in the whole maneuvering model, while the others are subordinate. This verify a standpoint once again that poor sensitive derivative gives bad estimation result [25,36].

Furthermore, the comparison between ISSI and ESSI are also carried out via the 25°/25° zigzag test and 30° turning circle maneuvering predictions, and the simulation results are shown in Figs. 7–10. Even though the identification results are extremely unsatisfactory, it is worth noting that the maneuvering simulations, which are based on the coefficients identified with ESSI are also satisfactory in some extent, especially for the turning circle maneuver. The main reason for the favorable maneuvering prediction is that the linear hydrodynamic derivatives, which have higher identification accuracy and sensitivity values, play a dominant role on the maneuvering model and ensure the precision of the maneuvering prediction.

Comparing Tables 1–3 with Tables 4–6 and Figs. 3–6 with Figs. 7–10, we can find that the identification results and the maneuvering predictions based on ISSI are much better than ESSI-based approaches.

Our observations from the comparisons of the identification results are as follows,

Table 7
Identified hydrodynamic derivatives of yaw motion with ESSI ($\times 10^{-5}$).

Sway	N'_0	N'_{0u}	N'_{0uu}	N'_v	N'_r	N'_δ	N'_{vvv}	$N'_{\delta\delta\delta}$
Original	3	6	3	−264	−166	−139	1636	45
Identified	2	−20	−172	−232	−167	−138	3081	62
Error (%)	28	436	5855	12	1	1	88	38

Sway	N'_{vvr}	$N'_{vv\delta}$	$N'_{v\delta\delta}$	$N'_{\delta u}$	N'_{vu}	N'_{ru}	$N'_{\delta uu}$
Original	−5483	−489	13	−278	−264	−166	−139
Identified	−4405	122	−418	−152	−90	−92	537
Error (%)	20	125	3318	45	66	44	486

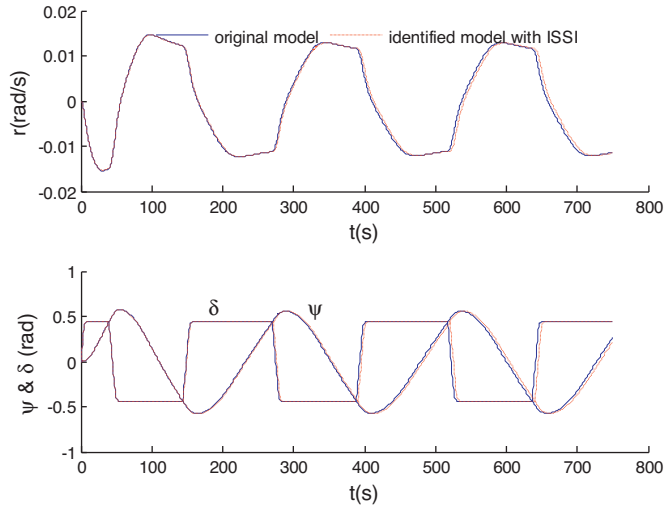

Fig. 4. Time histories of yaw rate, rudder and yaw angles of 25°/25° zigzag test.

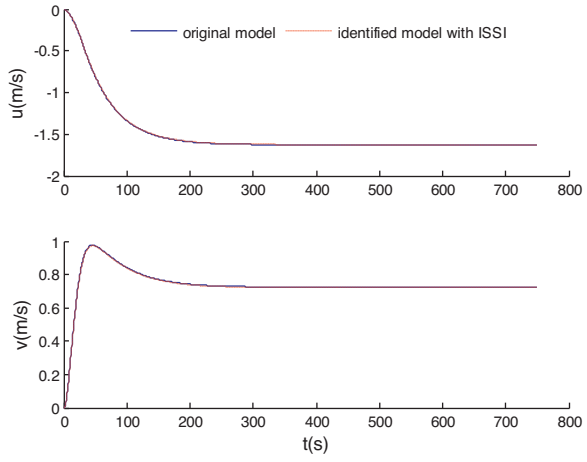

Fig. 5. Time histories of surge and sway velocities of 30° turning circle test.

1) Part of hydrodynamic derivatives, especially the linear ones, can be accurately approximated either ISSI or ESSI is used for the construction of in–out sample pairs.
2) For the rest derivatives, most of them can be identified with acceptable precision with ISSI, while most of the ESSI-based identification results have big errors.
3) Although some derivatives such as $Y'_{vv\delta}$ and Y'_{0uu} are always identified with high errors, the overall amplitude variation of the ISSI-based identification results is much smaller than ESSI-based identification results.

Our observations from the maneuvering predictions are as follows,

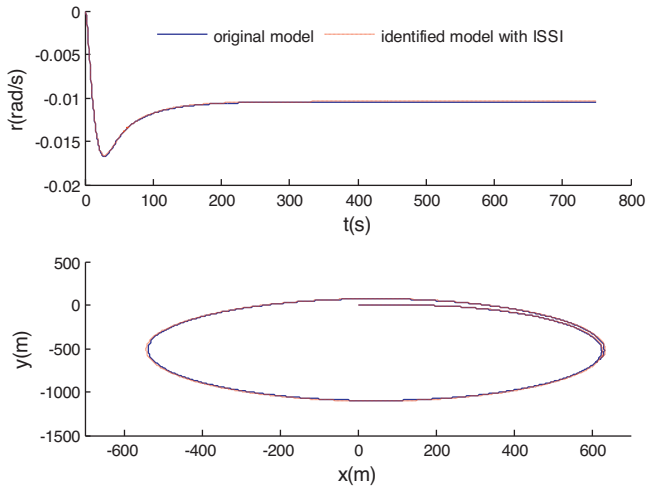

Fig. 6. Time histories of yaw rate and motion trajectory of 30° turning circle test.

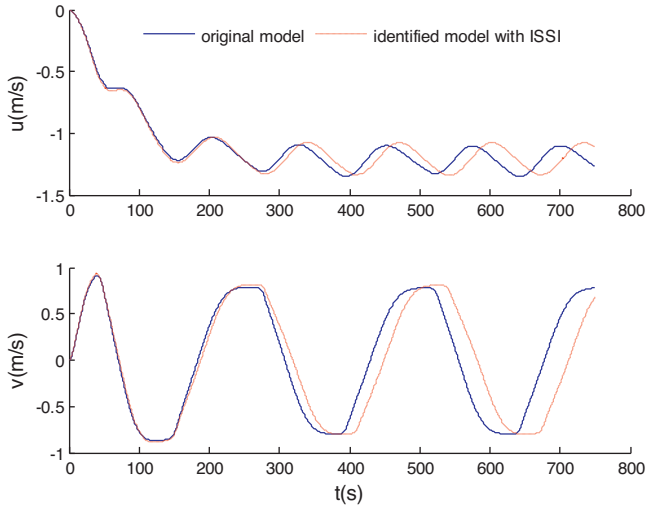

Fig. 7. Time histories of surge and sway velocities of 25°/25° zigzag test.

1) The maneuvering predictions based on the ISSI-based identification results are consistent with those based on the original model, while the predictions based on the ESSI-based results are slightly inferior.
2) Both ISSI and ESSI-based identification results are able to commendably predict the turning circle maneuver, while the ESSI-based approach cannot accurately predict the results of zigzag maneuver.

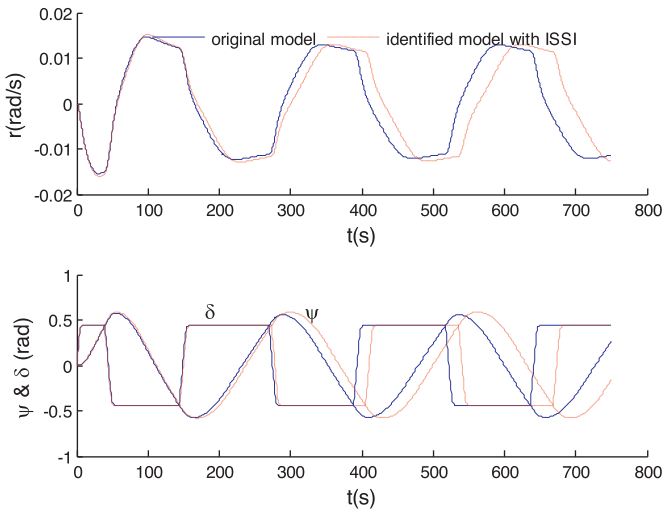

Fig. 8. Time histories of yaw rate, rudder and yaw angles of 25°/25° zigzag test.

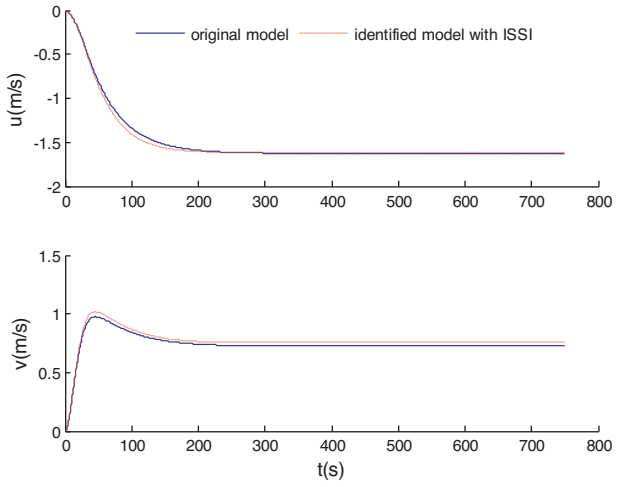

Fig. 9. Time histories of surge and sway velocities of 30° turning circle test.

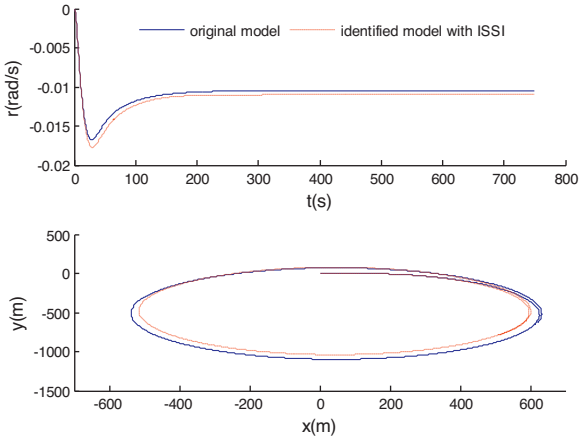

Fig. 10. Time histories of yaw rate and motion trajectory of 30° turning circle test.

5. Conclusions

This paper presents the parametric identification modeling of ship maneuvering motion with conventional ESSI and proposed ISSI by using LS-SVM. Based on the sample dataset obtained from 15°/15° zigzag maneuver, the hydrodynamic derivatives in Abkowitz model are all identified and then used for maneuvering prediction including 25°/25° zigzag and 30° turning circle maneuvers. The comparison of the identification results and maneuvering predictions suggest that the proposed ISSI outperform the conventional ESSI. The proposed ISSI can be used as the accurate modeling of ship maneuvering.

Acknowledgements

This work was supported by the National Natural Science Foundation of China (Grant Nos.: 50979060, 51279106 and 51409054) and Fundamental Research Funds for the Central Universities (Grant No.: HEUCF150118).

Appendix A. Supplementary data

Supplementary data associated with this article can be found, in the online version, at doi:10.1016/j.apor.2015.06.007

References

[1] Rhee KP, Lee SY, Sung YJ. Estimation of manoeuvring coefficients from PMM test by genetic algorithm. In: Proceedings of the international symposium and workshop on force acting on a manoeuvring vessel. 1998. p. 77–87.
[2] Smallwood DA, Whitcomb LL. Adaptive identification of dynamically positioned underwater robotic vehicles. IEEE Trans Control Syst Technol 2003;11(4):505–15.
[3] Abkowitz MA. Measurement of hydrodynamic characteristic from ship maneuvering trials by system identification. SNAME Trans 1980;88:283–318.
[4] Hwang WY [Ph.D. thesis] Application of system identification to ship maneuvering. Cambridge, MA: MIT; 1980.
[5] Källström CG, Åström KJ. Experiences of system identification applied to ship steering. Automatica 1981;17(1):187–98.
[6] Zhou WW, Blanke M. Identification of a class of nonlinear state-space models using RPE techniques. IEEE Trans Autom Control 1989;34(3):312–6.
[7] Åström KJ, Källström CG. Identification of ship steering dynamics. Automatica 1976;12(1):9–22.
[8] Tiano A, Sutton R, Lozowichi A, Naeem W. Observer Kalman filter identification of an autonomous underwater vehicles. Control Eng Pract 2007;15(6):727–39.
[9] Bhattacharyya SK, Haddara MR. Parametric identification for nonlinear ship maneuvering. J Ship Res 2006;50(3):197–207.
[10] Perez T, Fossen TI. Practical aspects of frequency-domain identification of dynamic models of marine structures from hydrodynamic data. Ocean Eng 2011;38(2–3):426–35.
[11] Banazadeh A, Ghorbani MT. Frequency domain identification of the Nomoto model to facilitate Kalman filter estimation and PID heading control of a patrol vessel. Ocean Eng 2013;72:344–55.
[12] Haddara MR, Wang Y. Parametric identification of maneuvering models for ships. Int Shipbuild Prog 1999;46(445):5–27.
[13] Moreira L, Guedes Soares C. Dynamic model of manoeuvrability using recursive neural networks. Ocean Eng 2003;30(13):1669–97.
[14] van de Ven PWJ, Johansen TA, Sørensen AJ, Flanagan C. Neural network augmented identification of underwater vehicle models. Control Eng Pract 2007;15(6):715–25.
[15] Rajesh G, Bhattacharyya SK. System identification for nonlinear maneuvering of large tankers using artificial neural network. Appl Ocean Res 2008;30(4):256–63.
[16] Zhang XG, Zou ZJ. Black-box modeling of ship manoeuvring motion based on feed-forward neural network with Chebyshev orthogonal basis function. J Mar Sci Technol 2013;18:42–9.
[17] Mahfouz AB, Haddara MR. Effect of the damping and excitation on the identification of the hydrodynamic parameters for an underwater robotic vehicle. Ocean Eng 2003;30(8):1005–25.
[18] Xu F, Zou ZJ, Yin JC, Cao J. Identification modeling of underwater vehicles' nonlinear dynamics based on support vector machines. Ocean Eng 2013;67:68–76.
[19] Vapnik VN. The nature of statistical learning theory. New York, USA: Springer Verlag; 1995.
[20] Amari S, Wu S. Improving support vector machine classifiers by modifying kernel functions. Neural Netw 1999;12(6):783–9.
[21] Lee YJ, Mangasarian OL. SSVM: a smooth support vector machine for classification. Comput Optim Appl 2001;20(1):5–22.
[22] Luo WL, Zou ZJ. Parametric identification of ship maneuvering models by using support vector machines. J Ship Res 2009;53(1):19–30.
[23] Zhang XG, Zou ZJ. Identification of Abkowitz model for ship manoeuvring motion using ε-support vector regression. J Hydrodyn 2011;23(3):353–60.
[24] Zhang XG, Zou ZJ. Estimation of the hydrodynamic coefficients from captive model test results by using support vector machines. Ocean Eng 2013;73:25–31.

[25] Xu F, Zou ZJ, Yin JC, Cao J. Parametric identification and sensitivity analysis for autonomous underwater vehicles in diving plane. J Hydrodyn 2012;24(5):744–51.
[26] Xu F, Chen Q, Zou ZJ, Yin JC. Modeling of underwater vehicles' maneuvering motion by using integral sample structure for identification. J Ship Hydrodyn 2014;18(3):211–20.
[27] Ridao P, Tiano A, El-Fakdi A, Carreras M, Zirilli A. On the identification of non-linear models of unmanned underwater vehicles. Control Eng Pract 2004;12(12):1483–99.
[28] Avila JPJ, Donha DC, Adamowski JC. Experimental model identification of open-frame underwater vehicles. Ocean Eng 2013;60:81–94.
[29] Tian YJ, Bian XQ. Identification of hydrodynamic parameters of AUV with the total least squares method. Control Theory Appl 2006;25(2):4–7 (in Chinese).
[30] Fossen TI. Guidance and control of ocean vehicles. New York: John Wiley & Sons; 1994.
[31] Chislett MS, Strom-Tejsen J. Planar motion mechanism tests and full-scale steering and maneuvering predictions for a Mariner class vessel. Int Shipbuild Prog 1965;12(129):201–24.
[32] Suykens JAK, Vandewalle J, De Moor B. Optimal control by least squares support vector machines. Neural Netw 2001;14(1):23–35.
[33] Suykens JAK. Support vector machines and kernel-based learning for dynamical systems modeling. In: Proceedings of the 15th IFAC symposium on system identification, vol. 15, no. 1. 2009. p. 1029–37.
[34] Hwang WY. Cancellation effect and parameter identifiability of ship steering dynamics. Int Shipbuild Prog 1982;26:90–120.
[35] Xu F, Zou ZJ, Yn JC, Cao J. Sensitivity analysis of hydrodynamic derivatives for ship maneuvering. J Harbin Eng Univ 2013;6:669–73 [in Chinese].
[36] Rhee KP, Kim K. A new sea trial method for estimating hydrodynamic derivatives. Ship Ocean Technol 1999;3(3):25–44.